Ultrafast dynamics in field-enhanced saturable absorbers

J. R. Karin, R. J. Helkey,[a] D. J. Derickson,[b] R. Nagarajan, D. S. Allin, J. E. Bowers, and R. L. Thornton[c]
Department of Electrical and Computer Engineering, University of California, Santa Barbara, California 93106

(Received 31 August 1993; accepted for publication 18 November 1993)

Absorption recovery dynamics of GaAs/AlGaAs field-enhanced waveguide saturable absorbers are studied by pump-probe differential transmission measurements. We compare the response of bulk and single quantum well absorbers at different reverse bias levels and pump powers, and find an ultrafast transient in the response, followed by a slower rise before the final recovery. The absorption fully recovers after a few picoseconds, which is an important result for mode-locked lasers.

Bulk and quantum well semiconductors have been used as saturable absorbers to generate short pulses in color center,[1] erbium-doped fiber,[2] dye,[3] solid state,[4] and semiconductor[5] laser systems. In these applications, damage sites or traps are created in the semiconductor by ion implantation in order to reduce the absorption recovery time from nanoseconds to several picoseconds. In semiconductor diode lasers, saturable absorber sections have been formed by implantation through one of the mirrors.[6] A more robust technique for passive and hybrid mode locking of diode lasers involves incorporating separately biased saturable absorber waveguide sections in a multisection laser.[7] The saturable absorber sections are typically p-i-n structures operated under reverse bias. Devices of this type have produced pulses of 0.6 ps, at repetition rates up to 350 GHz.[8] Saturable absorbers also play an important role in the elimination of multiple pulses in external cavity mode-locked diode lasers.[9] In order to produce a stable train of short pulses at these microwave and millimeter-wave repetition rates, the absorption recovery must be fast enough to recover on each round trip in the cavity. Understanding the dynamics of the saturable absorbers is necessary for laser design optimization. It is also important to understand the mechanisms of the nonlinear absorption properties of waveguide structures and the inherent limits to their recovery times. In this letter we present an experimental study of the bleaching and recovery dynamics of these field-enhanced waveguide saturable absorbers for different bias conditions and discuss the implications of the results for mode-locked diode lasers.

A schematic drawing of the experimental setup for measuring bulk and quantum well saturable absorbers is shown in Fig. 1, along with the basic layer structure of the devices. The active region consists of 820 Å of $Al_{0.04}Ga_{0.96}As$ in the bulk device, or a 150 Å quantum well with 720 Å undoped $Al_{0.3}Ga_{0.7}As$ barriers in the single quantum well (SQW) device. The lateral waveguide is formed by impurity-induced disordering.[10] A section of waveguide ~100 μm long is used for the measurements; in actual multisegment devices the saturable absorber section length is typically ~16 μm. Both end facets are antireflection coated with SiN_x, and have a residual facet reflectivity of 10^{-3}. The device is biased through a bias tee and the high frequency port is terminated in a 50 Ω sampling head and high-speed sampling oscilloscope. We measure differential transmission using a pump-and-probe technique with pulses of ~150 fs from a mode-locked $Ti:Al_2O_3$ laser. The center wavelength is adjusted to the lasing wavelength of the diode laser when it is mode-locked. We estimate the pump pulse energy coupled into the device to be 5–20 pJ. The pulse energy in a mode-locked diode laser is typically a few pJ. While the pulse energy is a factor of 2–10 higher in our measurements, the absorber in these experiments is also nearly ten times as long as the absorber sections in an integrated device, and more energy is needed to saturate it.

The pump and probe beams are orthogonally polarized to eliminate coherence effects. Measurements done under forward bias result in a change of sign of the differential transmission signal, verifying that the transients seen in the data are not coherence artifacts. We align the beams to the waveguide by using the device as a reverse-biased p-i-n photodiode and observing the photocurrent. We maximize the signal to achieve the best coupling into the waveguide, and find the approximate zero time-delay point by overlapping in time the photocurrent pulses from the pump and probe beams on the sampling oscilloscope. We assume that the exact $t=0$ point is given by the position of the initial transient in the data.

In these experiments we measure the transmission of the probe pulse as a function of the time delay between the pump and probe. The transmitted probe beam is effectively a measure of the electron population in the conduction band at the

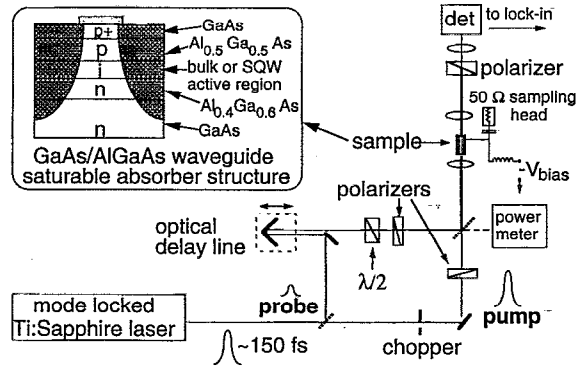

FIG. 1. (a) Device structure and (b) experimental configuration for pump-probe measurements of field-enhanced GaAs/GaAlAs waveguide saturable absorbers formed by impurity-induced disordering.

[a]Currently at University of Tokyo, Institute of Industrial Science, 7-22-1 Roppongi, Japan.
[b]Currently at Hewlett–Packard Corporation, Santa Rosa, CA 95403.
[c]Xerox Palo Alto Research Center, Palo Alto, CA 94304.

 0003-6951/94/64(6)/676/3/$6.00

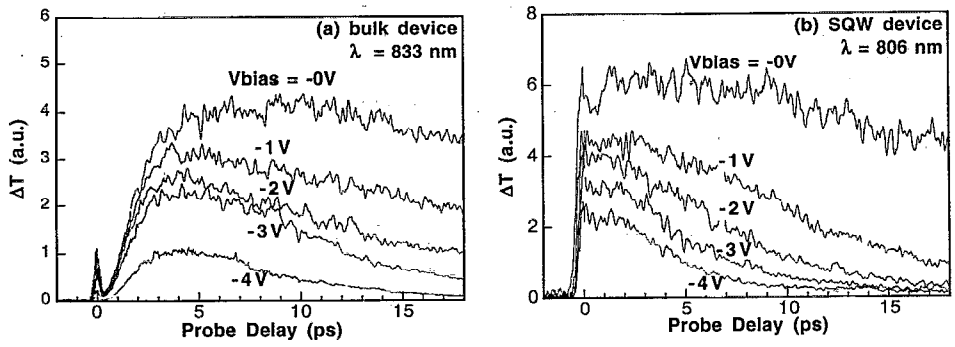

FIG. 2. Differential transmission data for (a) bulk and (b) SQW waveguide saturable absorbers, for different reverse bias values.

probe energy. We would expect to see a very fast rise in the transmission at zero delay corresponding to the bleaching of the device by the strong pump pulse, followed by a decay as the photogenerated carriers are swept out of the intrinsic region and the absorption recovers. Differential transmission data for bulk and SQW devices at different reverse bias values are shown in Fig. 2. In addition to the expected transmission change, we observe a very fast initial transient, on the order of 150 fs. This transient is followed by a slower rise that peaks after a few picoseconds, and finally an exponential recovery that depends on the reverse bias. For all values of bias the final $1/e$ recovery time is quite fast, typically less than 15 ps, and is as short as 4 ps at high bias levels. The bias dependence of the final recovery time is plotted in Fig. 3. There is a monotonic decrease in recovery time with increasing bias, as expected due to reduced emission time across the heterojunction and shorter transit times across the undoped region. The dependence is modeled well by an exponential function, which is qualitatively indicative of thermionic emission.

Existence of ultrafast features indicate that the actual absorption dynamics and mechanism of carrier removal in these experiments is more complicated than simple drift and thermionic emission of photoexcited carriers. The fast transient, the slower second rise time and the bias-dependent recovery are results of several physical mechanisms: electroabsorption, band-gap renormalization, carrier–carrier and carrier–phonon scattering, heating of the carriers by the field and intervalley scattering. In addition, the large space charge generated by the photoexcited carriers will act to screen the applied and built-in field. A complete analysis of these effects is beyond the scope of this letter. However, we will compare results from different reverse bias values, device structures, and pump powers vis á vis these mechanisms to gain an understanding of the important features in the data.

In addition to changing the final sweepout time, changing the bias will affect any electroabsorption effects. As seen in Fig. 2, apart from the final recovery time the main effect of changing the bias voltage is a change in the overall signal level. At higher bias, the initial absorption is higher due to (dc) electroabsorption, so the overall transmitted signal is lower. There does not appear to be any ultrafast electroabsorption effects that change with bias. Even at high bias, the field in the absorbing region is completely screened after ~100 fs and is not restored until the carriers are swept into the contacts, so the spatial carrier distribution remains fairly uniform over the time scale of the fast transient and subsequent rise. Thus the dynamics are due more to changes in the energy distribution rather than the spatial distribution.

Electroabsorption causes a blue shift in the absorption edge once the field collapses, which could account for the second rise in the data. The difference between the spatial carrier distribution in bulk and SQW device serves as a probe of the importance of this effect. In a SQW device the absorbing region is much thinner than in a bulk device. The carriers are swept out of the absorbing region faster, but they still must traverse the barriers before reaching the contacts, where they screen the fields in the active region. This should lead to a larger second peak in a SQW device if the blueshift due to electroabsorption is the dominant effect. Data from pump-probe measurements of SQW saturable absorbers are shown in Fig. 2(b). While qualitatively similar to the bulk data in Fig. 2(a), the initial bleaching does not recover as completely. The second peak is smaller in the SQW data than in the bulk, indicating that electroabsorption is not responsible for the ultrafast features.

Carrier–carrier scattering should be comparable in bulk and quantum well structures, and the presence of the fast initial transient in both sets of data suggests that this is a significant effect.[11] The high initial carrier density undergoes scattering within the first 100 fs, causing the fast transient. In addition, the field accelerates the carriers to higher energies, many past the threshold for intervalley scattering. Once the field collapses, the more energetic carriers scatter back down

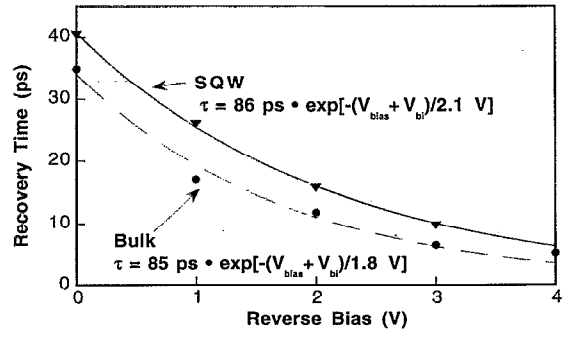

FIG. 3. Final absorption recovery time vs reverse bias for bulk and SQW waveguide saturable absorbers. Dashed and solid lines are fits to the data.

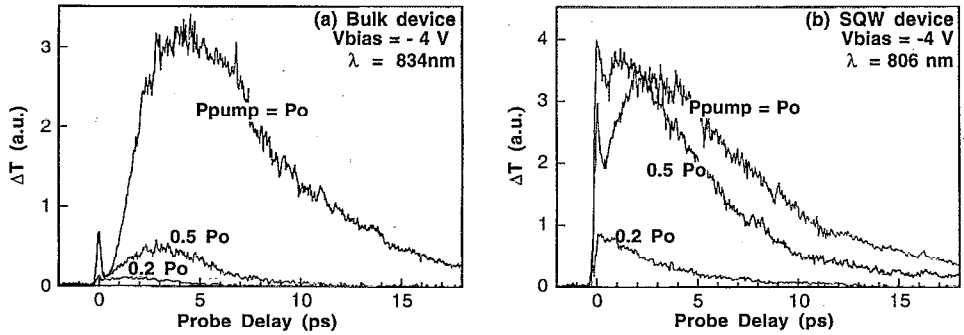

FIG. 4. Comparison of differential transmission data at three different pump power levels in (a) bulk and (b) SQW saturable absorbers. In each case, P_0 corresponds to approximately 2 mW (at 109 MHz) being coupled into the device.

to the probe energy, leading to the second transmission peak. Intervalley scattering has a smaller effect in the SQW device, because the quantum well in these devices is shallow relative to the threshold energy for intervalley scattering. Once the carriers have been accelerated by the field, real-space transfer into the barriers will be more likely than intervalley scattering, thereby reducing the amplitude of the second peak.

Figures 4(a) and 4(b) compare data from the bulk and SQW saturable absorbers at three different pump powers. The relative amplitudes of the fast transient and slower second peak are quite different in the three curves. With lower power, the second peak is much smaller relative to the initial fast transient, and rises faster than with high power, the delay between the initial bleaching and the second peak decreases dramatically with decreasing pump power. In the SQW device, at the lowest pump power the initial "spike" disappears; there is a sharp initial rise and an exponential-like decay, with no fast fall time and no slow rise to a second peak. These results are indicative of band-gap renormalization (BGR). BGR shrinks the band gap when the carrier density is high, increasing the absorption. This could be contributing to the fast transient fall time, since this feature disappears at low powers. In addition, at low power there is much less space charge, so there is little screening of the applied field and the removal of photoexcited carriers from the i region is much more efficient. More of the carriers excited to higher energies will be swept out before they have a chance to scatter into satellite valleys or back to the probe energy, hence the decrease in magnitude of the second peak with decreasing pump power.

The data have important implications for mode-locked semiconductor lasers. The short recovery times measured indicate that high frequency mode locking with these devices is possible. The recovery time is also important in determining the placement of the saturable absorber with respect to the output mirror to take advantage of colliding pulse effects and optimize the pulse width and/or output power.[12] We have successfully fabricated monolithic and external cavity mode-locked lasers containing saturable absorber sections in this material. Pulses of 2.8 ps were generated using an absorber length of 16 μm.[7] An absorption recovery time of 4 ps translates to a maximum repetition rate in excess of 250 GHz. The recovery time of the saturable absorber also indicates its ability to suppress multiple pulses in an external cavity mode-locked diode laser. With an absorption recovery time of 10 ps, secondary pulses can be suppressed in a diode with an internal roundtrip time of 10 ps. Multiple pulses were suppressed in a device mode-locked at a repetition rate of 5 GHz, with a total diode length of 500 μm and a saturable absorber length of 16 μm,[9] and a saturable absorber bias of -1.5 V. Under these conditions the pulsewidth was 2.9 ps, and the peak power was 0.25 W.

In summary, we have measured the absorption recovery dynamics in GaAlAs waveguide saturable absorbers. The absorption is fully recovered within several picoseconds in a 100 μm device. There is a subpicosecond dynamic with rise and fall times <150 fs which we attribute to a combination of a number of physical effects. Our experiments indicate that BGR, carrier–carrier scattering, and photon scattering are responsible for the ultrafast absorption transient. This transient should be useful for very high speed mode locking, and in fact it might be responsible for some of the high frequency mode-locking results that have been achieved.

We gratefully acknowledge Alan Mar and Thomas Reynolds for coating and mounting the devices, and Dan Cohen, Katie Hall, and Professor Herbert Kroemer for many helpful discussions. This work is supported by QUEST, a Science & Technology Center, Grant No. DMR91-20007.

[1] M. N. Islam, E. R. Sunderman, C. E. Soccolich, I. Bar Joseph, N. Sauer, T. Y. Chang, and B. I. Miller, IEEE, J. Quantum Electron. **QE-25**, 2454 (1989).
[2] M. Zirngibl, L. W. Stulz, J. Stone, J. Hugi, D. DiGiovanni, and P. B. Hansen, Electron. Lett. **27**, 1734 (1991).
[3] J. Feldmann, J. Sacher, and E. Gobel, Opt. Lett. **16**, 241 (1991).
[4] U. Keller, W. H. Knox, and G. W. t'Hooft, IEEE J. Quantum Electron. **QE-28**, 2123 (1992).
[5] J. P. van der Ziel, W. T. Tsang, R. A. Logan, R. M. Mikulyak, and W. M. Augustyniak, Appl. Phys. Lett. **37**, 525 (1981).
[6] A. G. Weber, M. Schell, G. Fischbeck, and D. Bimberg, IEEE J. Quantum Electron. **QE-28**, 2220 (1992).
[7] D. J. Derickson, R. J. Helkey, A. Mar, J. R. Karin, J. G. Wasserbauer, and J. E. Bowers, IEEE J. Quantum Electron. **QE-28**, 2186 (1992).
[8] Y.-K. Chen and M. C. Wu, IEEE J. Quantum Electron. **QE-28**, 2176 (1992).
[9] D. J. Derickson, R. J. Helkey, A. Mar, J. R. Karin, J. E. Bowers, and R. L. Thornton, IEEE Photon, Technol. Lett. **PTL-4**, 333 (1992).
[10] R. L. Thronton, W. J. Mosby, and T. J. Paoli, IEEE J. Lightwave Technol. **LT-6**, 786 (1988).
[11] W.-Z. Lin, R. W. Schoenlein, J. G. Fujimoto, and E. P. Ippen, IEEE J. Quantum Electron **QE-24**, 267 (1988).
[12] R. J. Helkey, Ph.D. dissertation, University of California, Santa Barbara, 1993.